2007 IEEE International Conference on
Robotics and Automation
Roma, Italy, 10-14 April 2007

Realtime collision avoidance using a robot manipulator with light-weight small high-speed vision systems

Sho Morikawa, Taku Senoo, Akio Namiki and Masatoshi Ishikawa

Abstract— **This paper describes a new realtime collision avoidance algorithm for a robot manipulator based on a new visual servo control. In the proposed algorithm, it is not necessary to compute the 3D position of the obstacle. Further, the manipulator can avoid the fast moving obstacle. The developed system uses several small light-weight high-speed vision chips placed on the surface of the robot manipulator. Experimental results of avoiding high-speed motion are shown.**

I. Introduction

Recently, the need for a robot that collaborates with humans has increased in both the industrial setting, such as in cell production work, and in home use. When a robot works in close proximity to a human, human safety is a big problem. A robot must not hurt a human, and it must have the ability to stop or avoid collision.

In order to achieve such collision avoidance capability, it is necessary to measure the approach of an obstacle in realtime using a displacement sensor. Some researches have used an ultrasonic sensor for this purpose, but this approach is not appropriate for collision avoidance in complex robot mechanisms, because it can not obtain global information on an obstacle [7]. Other researches have used a vision for collision avoidance. K. Hosoda et al. proposed a trajectory generator for avoidance of static obstacles [6]. N. Mansard et al. presented a control law that achieves the main task and avoidance simultaneously by visual servoing [3].

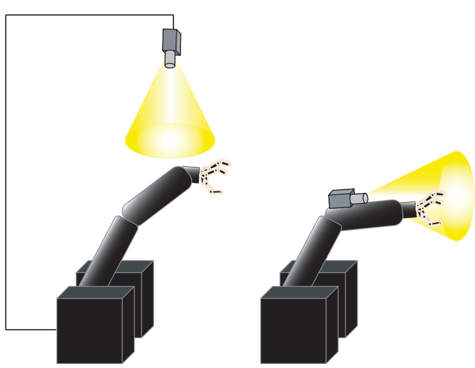

Fig. 1. Fixed camera type (left) and Eye-in-hand type (right)

One of the most serious problems of a vision sensor is the processing time. In usual CCD cameras, the vision sampling rate is 30 Hz. This is too slow for avoidance motion. In order to solve this problem, 1 kHz high-speed vision chip system

S. Morikawa, T. Senoo, A. Namiki, and M. Ishikawa are with Dept. of Information Physics and Computing, Univ. of Tokyo, 7-3-1 Hongo, Bunkyo-ku, Tokyo 113-8656, Japan. morikawa@k2.t.u-tokyo.ac.jp

Fig. 2. Multiple vision sensor network on the robot arm

has been developed [4]. The architecture is a massive parallel processing system, in which each pixel is connected with one processing element. Using this high-speed vision system, high-speed motion has been achieved by several researchers. A. Namiki et al. presented a control law for high-speed visual servoing [2]. Y. Nakabo et al. proposed a scheme for visual based control in realtime [1]. D. Ebert et al. proposed a safety measure using a high-speed vision [5].

In the previous works [1], [3], [5], and [6], and as shown in Fig.1(left), the camera head was placed outside of the robot, because of the large size of the camera head. We call this the ”fixed camera setting”. This setting has the advantage of measurement over a wide area of both robot and surrounding environment. If there is another obstacle between the manipulator and camera, the vision cannot detect collision.

On the other hand, as shown in Fig.1(right), the ”eye on hand” setting is popular in visual servoing. This setting has the advantageous in collision avoidance problem. By arranging cameras at appropriate positions on the robot, the vision can detect possible collision without disturbance from other objects. The size of a recent camera heads of a vision chip systems is small, and they are sufficiently light weight to be able to be mounted on the end effector of a manipulator. In the future, small high-speed vision systems will have a low price. Once this is achieved, a vision sensor network can be mounted on the robot surface as shown in Fig.2, and this network can be used for detection and collision avoidance, as well as realtime recognition of the environment, and so

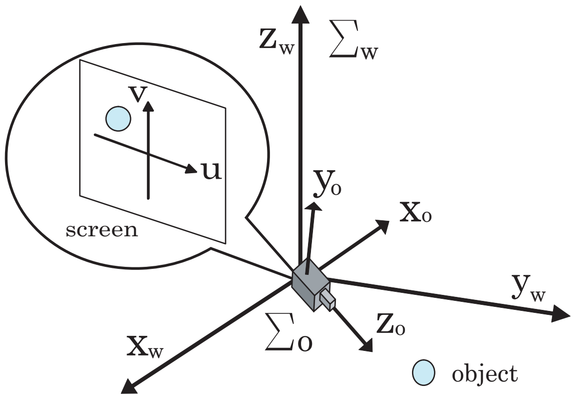

Fig. 3. Coordinate system of a camera

on.

In this paper, we propose a collision avoidance system in which two light-weight small high-speed camera heads are placed on a robot manipulator. For this system, we propose a new realtime collision avoidance algorithm based on visual servoing control. The proposed system is a first step of a robot system with a vision-sensor-network. We expect the system will be extended to collision avoidance with multi-vision systems.

II. VISUAL SERVOING FOR HIGH-SPEED TARGET TRACKING

A. Traditional visual servoing control for target tracking

Figure 3 shows a general visual servoing system, in which the position and the orientation of the camera are controlled by visual information. In Fig.3, Σ_w is the world coordinate system and Σ_o is the camera coordinate system fixed on the camera. The vector $u = [u, v]^T \in \mathbb{R}^2$ is the position of a target on the image plane, and f is focus length. The vector $x_w \in \mathbb{R}^3$ and $x_o \in \mathbb{R}^3$ are the position of the object in the Σ_w and Σ_o , respectively. These variables satisfy the following equations.

$$u = f \cdot \begin{pmatrix} \frac{x_o}{z_o} \\ \frac{y_o}{z_o} \end{pmatrix} \quad (1)$$

$$x_w = R x_o + p \quad (2)$$

where $R \in \mathbb{R}^{3\times 3}$ and $p \in \mathbb{R}^3$ represent the rotation matrix and transfer vector, respectively. And the vector $\theta = [\theta_1, \theta_2, \ldots, \theta_n] \in \mathbb{R}^n$ is the joint angles.

Assume that $\dot{x}_w = 0$, namely that the target is stationary. From the differentials of Eqn (1) and (2), we get

$$\dot{u} = f \cdot \begin{pmatrix} \frac{1}{z_o} & 0 & -\frac{x_o}{z_o^2} \\ 0 & \frac{1}{z_o} & -\frac{y_o}{z_o^2} \end{pmatrix} \dot{x}_o \quad = A\ \dot{x}_o \quad (3)$$

and

$$\dot{x}_w = \frac{\partial (R x_o)}{\partial \theta} \dot{\theta} + R\dot{x}_o + \frac{\partial p}{\partial \theta} \dot{\theta} \quad = \quad B\dot{\theta} + R\dot{x}_o = 0 \quad (4)$$

where

$$B = \frac{\partial (R x_o)}{\partial \theta} + \frac{\partial p}{\partial \theta} \quad (5)$$

Using the inverse of Eqn.(3), the velocity control input of the camera is computed as follows.

$$\dot{\theta} = -J^{\dagger} \dot{u} \quad , \quad J = A R^T B \quad (6)$$

where the operator "†" means the pseudo inverse.

In this equation, the relationship between $\dot{u}$ and $\dot{\theta}$ is linear, and it is controlled only by visual information. Also if some disturbance is included in the Jacobian J, the positional error of u converges to zero. On the other hand, this standard visual servoing method has several problems in high-speed control. First, the depth z_o is included in the Jacobian J. In general, it is difficult to acquire the depth information using only one vision. Even with stereo vision, it is difficult to compute the depth correctly. For this reason, the feedback gain can not be given exactly. Next, it is assumed that the target is static or quasi-static, $\dot{x}_w = 0$. In a typical tracking task, a target is moving. If the speed of the moving target is rapid, the usual visual servoing method does not work well.

B. New visual servoing control for high-speed target tracking

In order to solve the two problems mentioned above, we develop a new visual servoing control in which we introduce features invariant to the depth information are introduced.

Assume that $p = 0$. This means that the motion of the camera consists of only rotation. Then we define a feature vector $\alpha \in \mathbb{R}^2$ as follows.

$$\alpha = \begin{pmatrix} \alpha \\ \beta \end{pmatrix} \quad (7)$$

$$\alpha = \frac{y_w}{x_w} = \frac{r_{21}u + r_{22}v + r_{23}f}{r_{11}u + r_{12}v + r_{13}f} \quad (8)$$

$$\beta = \frac{z_w}{x_w} = \frac{r_{31}u + r_{32}v + r_{33}f}{r_{11}u + r_{12}v + r_{13}f} \quad (9)$$

where r_{ij} is the ij-element of the Rotation matrix R.

The feature α can be calculated with only one vision, because it does not include the depth information z_o. For this reason, it is not necessary to compute the 3D position of the target. The feature α can not be computed if the denominator of α is 0,namely, $x_w = 0$. However it is symmetric, so we can replace the denominator with the other variables, y_w or z_w. The new feature can be used in the same way.

The feature α can be expressed as a function of the image feature u and the joint angle θ.

$$\alpha = \mathscr{F}(u, \theta) \quad (10)$$

Differentiating Eqn.(10),

$$\dot{\alpha} = F\dot{\theta} + G\dot{u} \quad (11)$$

where

$$F = \frac{\partial \mathscr{F}}{\partial \theta} = \begin{pmatrix} \frac{\partial \alpha}{\partial \theta_1} & \frac{\partial \alpha}{\partial \theta_2} & \cdots & \frac{\partial \alpha}{\partial \theta_n} \\ \frac{\partial \beta}{\partial \theta_1} & \frac{\partial \beta}{\partial \theta_2} & \cdots & \frac{\partial \beta}{\partial \theta_n} \end{pmatrix} \quad (12)$$

$$G = \frac{\partial \mathscr{F}}{\partial u} = \begin{pmatrix} \frac{\partial \alpha}{\partial u} & \frac{\partial \alpha}{\partial v} \\ \frac{\partial \beta}{\partial u} & \frac{\partial \beta}{\partial v} \end{pmatrix} \quad (13)$$

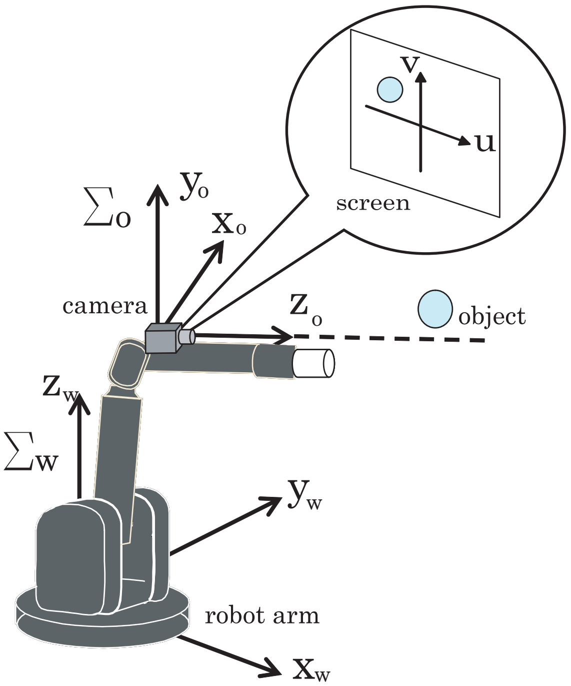

Fig. 4. Coordinate system

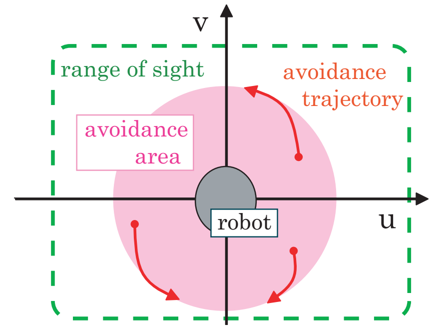

Fig. 5. Desired obstacle trajectory on the image plane

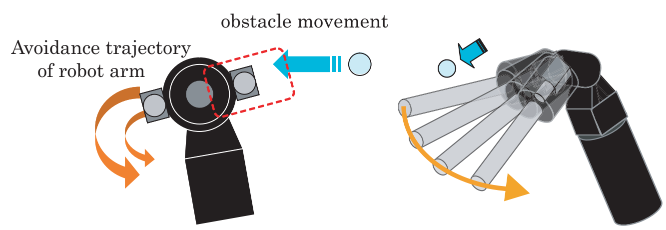

Fig. 6. Desired obstacle trajectory of the robot arm

Changing to a discrete expression, we obtain the desired joint angle at step $n+1$ as follows.

$$\theta_{n+1} = \theta_n - F^{\dagger}G(u_{n+1} - u_n) + F^{\dagger}(\alpha_{n+1} - \alpha_n) \quad (14)$$

In Eqn.(14), the desired image values u_d is substituted for u_{n+1}. And $\alpha_{n+1} - \alpha_n$ can not be computed at step n, so it is replaced by the previous step values $\alpha_n - \alpha_{n-1}$.

The proposed new visual servo control is suited for high-speed visual tracking because of the following two reasons. First, it is not necessary to acquire the depth information of the target, namely to compute the 3D position of the obstacle. Also, the feature α, the coefficient matrix F and G can be computed only by visual information. Next, the second term of Eqn.(14) is the compensation for motion of the target.

If the dimension of the joint space is two, F is a square matrix and $F^{\dagger}$ is equal to F^{-1}. In the next sections, we use 2-axis rotation joints $\theta = [\theta_1, \theta_2] \in \mathbb{R}^2$.

On the other hand, a demerit is the assumption that $p = 0$, namely the motion of a camera consists of only rotation. Because of this assumption, the application of the proposed method is limited to some special mechanisms. However, by setting vision at appropriate positions, it has a wide range of application.

III. Collision Avoidance Control

A. Setting of a camera

In the proposed visual servoing algorithm, we assume $p = 0$. However, in general this assumption is not satisfied. When the camera is set at the origin and only rotational motion is added, the assumption is satisfied. In order to solve the problem ($p = 0$), the camera should be set on the crosspoint of the rotation axes, such as the shoulder joint or the elbow joint. Also assume that rotational motions are mainly used for collision avoidance, and that translational motions are sufficiently small.

In the case that a robot arm has a structure similar to human beings, such as is illustrated in Fig.4, it is useful to use an elbow joint that consists of revolution and bending. In this situation, when we put cameras in the neighborhood of the elbow joint, we can take that $p = 0$ approximately. Generally, in the design of a robot manipulator, the crosspoint of rotation axes is often used to simplify the calculation of kinematics. So this assumption is not a special condition.

If the width of the robot is large, the camera can not be set just in the rotational center of the elbow joint. In this case, by setting two or three cameras around the elbow joint, the assumption $p = 0$ can be approximately achieved. In our case, we use two cameras, and the cameras are set at the both sides of the elbow joint.

B. Avoidance trajectory

Suppose that an obstacle is approaching from the side of the robot link. In this situation, an efficient avoidance trajectory is needed so that the trajectories of the joints are smooth. If the arm link steps back in the same direction as the obstacle motion, there is the possibility that the arm can not avoid the obstacle. On the other hand, if the arm link moves in a direction vertical to the obstacle motion, this motion is one of the most efficient avoidance motions. However, this motion is often a radical motion for the arm link, and there is the possibility of damage to the robot joints. In addition, it is necessary that the arm link avoids several obstacles which approach one after another. For this reason, the avoidance

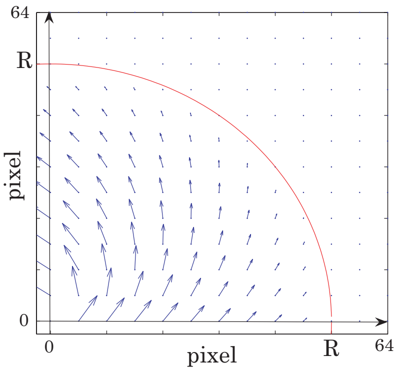

Fig. 7. Direction of the desired image value

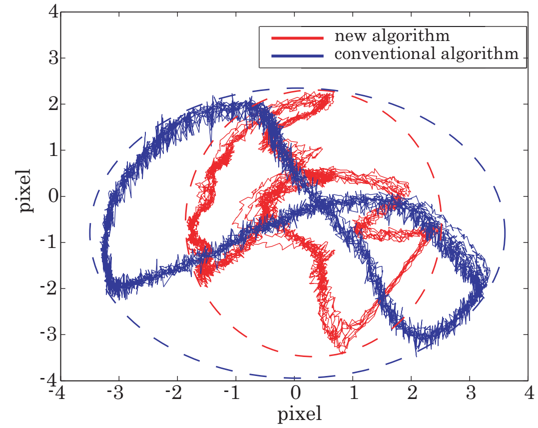

Fig. 9. Tracking of the hand of the metronome on the image plane

trajectory should be smooth, so that it can connect with the next avoidance trajectory.

In this paper, we propose a new avoidance strategy, as shown in Figs.5 and 6. In the proposed strategy, the arm link is controlled so that the obstacle describes a spiral on the image plane. The trajectory of the arm link also describes a spiral. The spiral trajectory can be connected smoothly with the other spiral trajectory, and the arm link can avoid obstacles quickly in succession. Because the trajectory is smooth, it does not damage the joints.

Let us obtain the desired image values, $u^d = [u_n^d, v_n^d]^T$, based on the above strategy. As shown in Fig.5, we set an avoidance area. Its center is set at the origin of the image plane, and its radius is R. If an obstacle enters this avoidance area, the arm link avoids the obstacle by describing a spiral. In this paper, the desired image values are given as an elastic movement related to the distance between the image center and the obstacle.

$$u_n = r\cos(\omega r) \quad , \quad u_n^d = (r+\Delta r)\cos(\omega(r+\Delta r)) \quad (15)$$

$$v_n = r\sin(\omega r) \quad , \quad v_n^d = (r+\Delta r)\sin(\omega(r+\Delta r)) \quad (16)$$

where $r = \sqrt{u_n^2 + v_n^2}$ is the distance between the robot and the obstacle on the image plane, ω is a constant gain, u_n and v_n represent current image values, and $\Delta r = k(R - r)$, where k is a constant gain. Figure 7 shows its example.

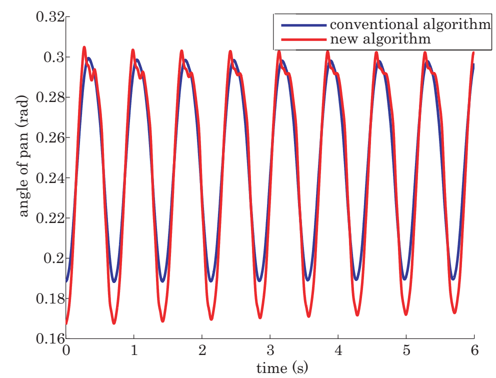

Fig. 10. Rotation of pan

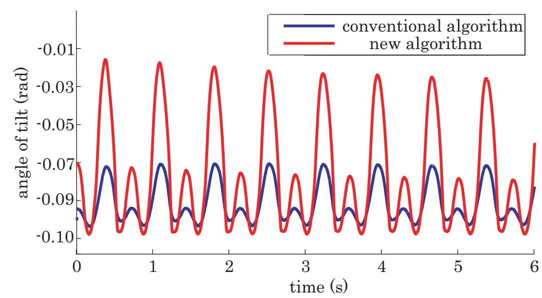

Fig. 11. Rotation of tilt

IV. Experiment using 2-axis active vision

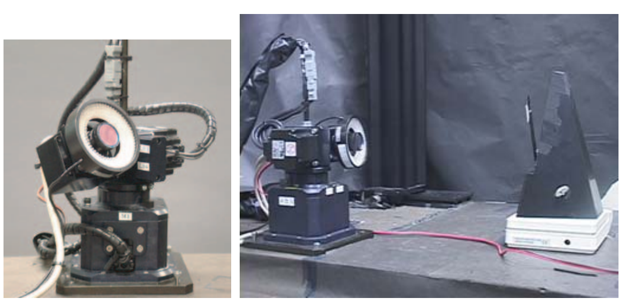

Fig. 8. Active vision system(left) and setting of experiment (right)

We will show experimental results of high speed tracking to make sure the effectiveness of our new visual servoing.

A. Two-axis active vision system

In the active vision system which has pan axis and tilt axis, the assumption $p = 0$ is satisfied. For this reason, it is useful to verify the effectiveness of the new visual servoing algorithm proposed in Section II. The total view of the system is shown in Fig.8 (left). It has the tilt axis and the pan axis, and a high-speed vision called CPV-III (column parallel vision system III made by Hamamatsu Photonics) is set on the active vision.

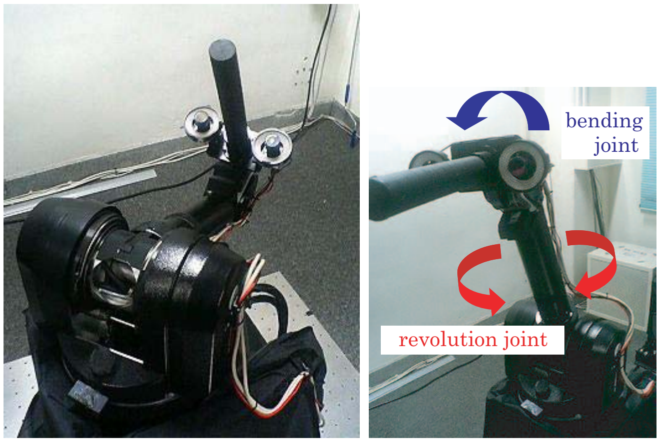

Fig. 12. Experimental system

CPV-III is a massively parallel vision system. It has 128×128 photo detectors with an all pixel parallel processing array based on vision chip architecture and an exclusive summation circuit for calculating moment values [4]. Because the visual processing is executed in parallel in the processing array, high-speed visual processing (moment detection, segmentation, etc.) is achieved within 1ms.

B. Experiment

The target is set on the hand of the metronome, which is installed in the front of the active vision at 30 cm distant as shown in Fig.8 (right). The hand of the metronome oscillates at a frequency of 1.4 Hz, and the active vision tracks the hand of the metronome. The active vision system is controlled so that the target is put in the center of its sight.

We compare our new visual tracking control with the traditional tracking control. The detailed control methods are explained in Section II. The feedback gains of PD control are appropriately set in each control method.

In Fig.9, the trajectory of the target on the image plane is shown. The blue line is the result of the traditional method, and the red line is the result of the new method. From viewing this figure it is clear that the tracking errors are smaller in the new method. In Fig.10 and Fig.11, the time response of the angle joints is shown. The amplitude of the trajectory based on the new method is larger. This means that the tracking control is more responsive. These results show that the new visual servo control is effective for high-speed tracking motion.

V. Experiment using a robot arm

Next, we will introduce experimental results of avoidance using a robot arm and high-speed visions.

A. Avoidance system

The total view of the system is shown in Fig.12. Two cameras of CPV-III are set on both sides of the elbow of the robot arm to cover the both right and left sides of it.

The robot arm is a wire-drive 4-axis manipulator made by Barrett Technology Inc.[8]. The maximum velocity of

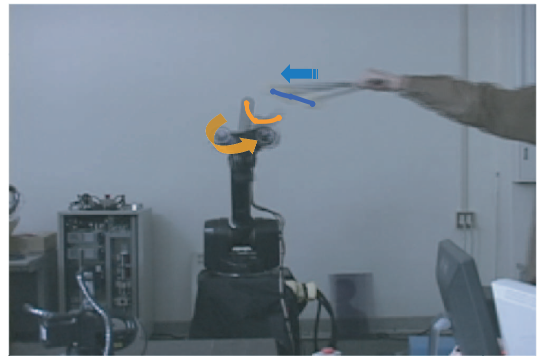

Fig. 13. Avoidance trajectory (piled)

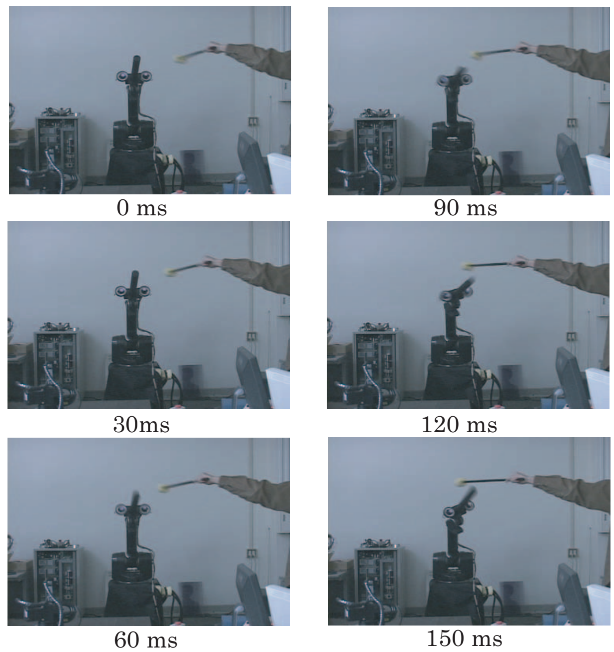

Fig. 14. Avoidance trajectory (continuous sequence)

the end-effector is 6 m/s, and the maximum acceleration is 58 m/s^2. The cycle time for visual processing and control processing is set at 1ms. This manipulator has four joints. However, in this study, only two joints at the elbow were used. The other joints were fixed. The realtime avoidance is achieved by the 2-axis rotation at the elbow.

As an obstacle, we use a yellow ball which is placed on the tip of a stick. A human moves the ball, and quickly brings it into the neighborhood of the robot arm. In our avoidance system, even if the ball goes out of camera sight during avoidance, the robot arm continues the avoidance motion as follow-through. This is because it is necessary to keep an appropriate distance between the arm and the obstacle. Moreover, if the arm moves as fast as the obstacle, suddenly stopping the arm may damage the joints in the robot.

B. Experiment

In Fig.14, the experimental result of avoidance is shown in a continuous sequence of images per 30 ms. An avoidance

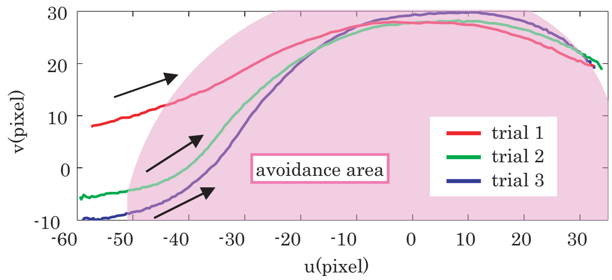

Fig. 15. Tracking of the obstacle on the image plane

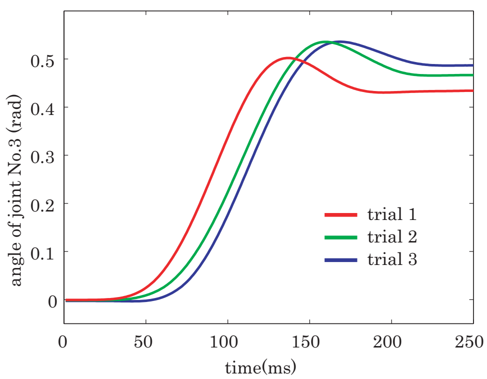

Fig. 16. Rotation of revolution joint

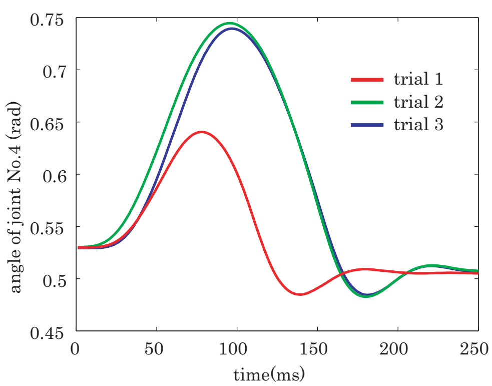

Fig. 17. Rotation of bending joint

motion is properly achieved in response to the position of the obstacle. Figure 13 is a composition of the photographs. The blue line shows the trajectory of the target, and the orange line is the trajectory of the tip of the arm. The robot arm avoids the obstacle, and finally goes behind of the obstacle.

Figure 15 shows the image plane of one camera. The red area shows the avoidance area. Any obstacle is removed from this red area. The lines are the trajectory of the target on the image plane. The obstacle is seen to be removed in a smooth spiral motion.

Figure 16 and 17 show the angles of the revolution and the bending at elbow. Same trial is described at the same colar in figures. Smooth joint motion is achieved, and follow-through motion is verified.

These results verify the effectiveness of the proposed avoidance system. The experimental result is shown as a movie on the web site [9].

C. Discussion

There are three important factors to improving the performance of avoidance. The first factor is the rate of visual feedback. In our experiment, the rate is 1 ms. If the rate is reduced, the performance is degraded.

The second factor is the range of sight. If the range is narrow, the motion become radical and dangerous. In order to solve this problem, it is important not only to set the camera in the appropriately position but also to select an appropriate lens.

The third factor is illumination. Because exposure time is very short in high-speed vision, it is necessary to use an appropriate illuminator. In this experiment, we used an LED ring which is set in front of the camera. It is important to achieve uniform illumination around the arm link.

VI. Conclusion

In this paper, we described and demonstrated a collision avoidance system in which two light-weight small high-speed camera heads were placed on a robot manipulator. For this system, we developed a new realtime collision avoidance algorithm based on visual servoing control.

This new visual servo control is suited to high-speed visual tracking for the following two reasons. First, it is not necessary to acquire the depth information of the target, namely to compute the 3D position of the obstacle. Next, the compensation for motion of the target is included. As a result, high-speed avoidance is achieved.

In the future, we will develop a vision sensor network that can be mounted on a robot surface as shown in Fig.2, and this network will be used for realtime detection and collision avoidance.

References

[1] Yoshihiro Nakabo, Masatoshi Ishikawa: "Visual Impedance Using Massively Parallel Vision System" The Robotics Society of Japan(2001) proceedings, Vol.19, No.8, pp.959-966
[2] Akio Namiki, Koichi Hashimoto, Masatoshi Ishikawa: "A Hierarchical Control Architecture for High-Speed Visual Servoing", The International Journal of Robotics Research, Vol.22, No.10-11, pp873-888 (2003)
[3] Nicolas Mansard, Francois Chaumette: "A new redundancy formalism for avoidance in visual servoing", In IEEE/RSJ Int. Conf. on Intelligent Robots and Systems (IROS2005), Vol 2, pp1694-1700
[4] Takashi Komuro, Idaku Ishii, Masatoshi Ishikawa, and Atsushi Yoshida: "High Speed Target Tracking Vision Chip", Int. Conf. on Computer Architecture for Machine Perception (Padova, 2000.9.11)/proceedings, pp.49-56
[5] Dirk Ebert, Takashi Komuro, Akio Namiki, Masatoshi Ishikawa: "Safe Human-Robot-Coexistence: Emergency-Stop Using a High-Speed Vision-Chip", IEEE / RSJ International Conference on Intelligent Robots and Systems (IROS2005)Proceedings, pp.1821-1826
[6] Koh Hosoda, Kenji Sakamoto, Minoru Asada: "Trajectory Generation for Obstacle Avoidance of Uncalibrated Stereo Visual Servoing without 3D Reconstruction", The Robotics Society of Japan(1997) proceedings, Vol.15, No.2, pp.290-295
[7] Toshio Tsuji, Makoto Kaneko: "Non-Contact Impedance Control for Redundant Manipulators", IEEE Transactions on Systems, Man, and Cybernetics -Part A: Systems and Humans (1999), Vol.29, No.2, pp.184-193
[8] http://www.barrett.com/
[9] http://www.k2.t.u-tokyo.ac.jp/fusion/Avoidance/